Photoneutron Production Cross Sections of Nickel and Silver*

D. S. FIELDER,† K. MIN, AND W. D. WHITEHEAD
University of Virginia, Charlottesville, Virginia
(Received 26 October 1967)

The least-structure solutions for the photoneutron production cross sections of natural nickel and silver were obtained from the neutron thresholds up to 25 MeV. The experimental results are compared with the theoretical dipole-strength distributions given by the dynamic collective theory and the theory of collective correlations.

I. INTRODUCTION

THE giant-dipole resonance of photon-absorption cross sections has been studied extensively in two regions of the periodic table, the light nuclei below $A=40$ and the heavier nuclei with large nuclear deformation. In the light nuclei, a relatively limited number of particle-hole configurations participate in the photoexcitation, producing a well-resolved discrete structure in the cross sections.[1] In the heavier nuclei, the effect of strong static nuclear deformation has been observed in the splitting of the giant-dipole resonance, in agreement with the classical hydrodynamical model.[2,3] In the past few years, there have been increasing indications that the higher-multipole vibrations play an important role in the photon absorption in nuclei, particularly in the intermediate and heavy spherical nuclei.[4–6] From the viewpoint of a simple shell model, the appearance of structure in the heavier spherical nuclei is rather unexpected because the dipole strengths are distributed among a sufficiently large number of levels to form a smooth, overlapping continuum. The structure observed in the photoneutron cross sections in some spherical nuclei has been interpreted as being due to the interaction between the dipole and quadrupole vibrations.

In the present work, the photoneutron production cross sections of two intermediate spherical nuclei, nickel and silver, were obtained from the neutron thresholds to 25 MeV using the least-structure analysis.[7] The experimental results, after the neutron-multiplicity corrections, were compared with the predictions of the dynamic collective theory for silver[5] and the theory of correlations for nickel.[6]

II. EXPERIMENTAL PROCEDURE

The collimated bremsstrahlung beam from the University of Virginia 70-MeV electron synchrotron was used in this experiment. After passing through a modified National Bureau of Standards ionization chamber[8,9] and a second collimator, the bremsstrahlung beam irradiated the samples which were placed along the beam axis at the center of a 4π Halpern-type neutron detector[10] made of paraffin and eight BF_3 counters. The neutrons from the sample were first slowed down in the intervening paraffin layers and were detected by a system of eight BF_3 counters placed concentrically about the beam axis at a radial distance of 13.5 cm. The detector was shielded from the extraneous neutron background by borated paraffin and cadmium sheets. The neutrons were counted for 700 μsec after a time delay of 20 μsec following each beam burst.

The efficiency of the neutron detector averaged about 2.5%. The neutron-detection efficiency and the response of the ionization chambers were checked regularly before each neutron-yield measurement using a 10-mCi Ra-Be source. Throughout the experiment, the fluctuation in the detection efficiency remained within 1% of its average value.

The nickel and silver samples were both cylindrical in form (nickel: 4.3 cm diam×5.2 cm; silver: 3.2 cm diam×2.4 cm), of natural abundance, and weighted 650 and 200 g, respectively. The abundance of the major contributing isotopes in each sample, and the (γ,n), $(\gamma,2n)$ threshold energies, are listed in Table I. For

TABLE I. Abundances of major isotopes, threshold energies, and level-density parameters.

Isotope	Abundance (%)	Threshold energies (MeV) (γ,n)	Threshold energies (MeV) $(\gamma,2n)$	Level-density parameter (MeV^{-1})[a]
Ni^{58}	68.0	12.2	22.5	5.49
Ni^{60}	26.2	11.4	20.4	5.49
Ag^{107}	51.4	9.4	17.1	10.00
Ag^{109}	48.6	9.2	16.4	10.00

[a] Taken from the semiempirical formula $a=A/10.9$ MeV^{-1} (a=level density, A=mass number) given in Ref. 14.

* Supported by the National Sicence Foundataion.
† Submitted in partial fulfillment of the requirements for the degree of Doctor of Philosophy at the University of Virginia.
[1] G. E. Brown, L. Castillejo, and J. A. Evans, Nucl. Phys. **22**, 1 (1961).
[2] M. Danos, Nucl. Phys. **5**, 23 (1958).
[3] K. Okamoto, Phys. Rev. **110**, 143 (1958).
[4] O. S. Fielder, J. LeTourneux, K. Min, and W. D. Whitehead, Phys. Rev. Letters **15**, 33 (1965).
[5] M. G. Huber, M. Danos, H. J. Weber, and W. Greiner, Phys. Rev. **155**, 1073 (1967).
[6] D. Dreschsel, J. B. Seaborn, and W. Greiner, Phys. Rev. **162**, 983 (1967).
[7] B. C. Cook, Nucl. Instr. Methods **24**, 256 (1963).
[8] J. S. Pruitt and S. R. Domen, Bur. of Stds. (U. S.) Monograph **48**, (1962).
[9] P. A. Flournoy, Ph.D. thesis, University of Virginia, 1962 (unpublished).
[10] P. A. Flournoy, R. S. Tickle, and W. D. Whitehead, Phys. Rev. **120**, 1424 (1960).

nickel, 20 neutron-yield curves were measured in 0.25-MeV increments from 10.25 to 25 MeV. For silver, a total of 18 yield curves were measured in 0.5-MeV steps from 9 to 25 MeV. For both cases, the background measurements were made in 0.5-MeV steps. These background yields were interpolated to obtain the background in 0.25-MeV steps for nickel. The statistical counting error in the yield was 0.3% for nickel and 0.6% for silver. From the net neutron yields, the least-structure solutions for the photoneutron production cross sections were obtained in 0.25-MeV bins for nickel and 0.5-MeV bins for silver.

It is well known that the analysis of the photonuclear yields functions without smoothing fails to give statistically significant cross sections in the higher-energy region above the giant-resonance peak. On the other hand, the least-structure analysis[7] of photonuclear yield is essentially a method for systematically smoothing the cross section, and this method of analysis is capable of producing the cross sections above the giant resonance. The least-structure cross sections $\sigma_i(i=1,2\cdots n)$ are the solutions to the following variational problem:

$$S(\sigma_i)=\text{Minimum}, \tag{1}$$

with the constraint

$$\chi^2=\sum_{i=1}^{n}[(\sum_{j=1}^{n}N_{ij}\sigma_j-y_i)/(\nabla y_i)^2]=n, \tag{2}$$

where N_{ij}'s are the bremsstrahlung matrix elements, y_i's are the reduced yields, ∇y_i's are the standard errors in the reduced yields, and n is the number of the yield points. The structure function $S(\sigma_i)$, while its form is arbitrary, must be such that its magnitude is small when the cross section is smooth and large when the cross section has many peaks and valleys. In order to study the effect of different structure functions on the cross-section results, two structure functions suggested by Cook[7] were used in the present data analysis.

$$S_1(\sigma_i)=\sum_{i=1}^{n-1}(\sigma_{i+1}-\sigma_i)^2, \tag{3a}$$

$$S_2(\sigma_i)=\sum_{i=2}^{n-1}(\sigma_{i+1}-2\sigma_i+\sigma_{i-1})^2. \tag{3b}$$

III. RESULTS

The photoneutron production cross sections for nicke are shown in Figs. 1 and 2, and Fig. 3 shows the results for silver. In each figure, the value of x^2 is an index of the degree of smoothing applied to the cross sections. $x^2=n$, where n is the number of the yield points ($n=60$ and 33 for nickel and silver, respectively), corresponds to optimum smoothing. $x^2<n$ and $x^2>n$ correspond to undersmoothed and oversmoothed solutions.

Figure 1 shows two solutions with optimum smoothing obtained for nickel using the two different smoothing functions, S_2 (upper curve) and S_1 (lower curve), defined in Eqs. (3a) and (3b). The main features of these two solutions are almost identical, indicating that the least-structure solutions are rather insensitive to the choice of smoothing function. The undersmoothed (upper curve) and the oversmoothed (lower curve) solutions shown in Fig. 2, obtained using S_2, retain the same main characteristics as the optimum solutions, although the undersmoothed solution reveals somewhat more pronounced structure. The optimum and an undersmoothed solution for silver obtained using S_2 are shown in Fig. 3. The horizontal bars in the results are the full widths at half maximum of the resolution function,[7] representing the effective energy interval over which the unsmoothed solutions are averaged to obtain the smoothed solutions.

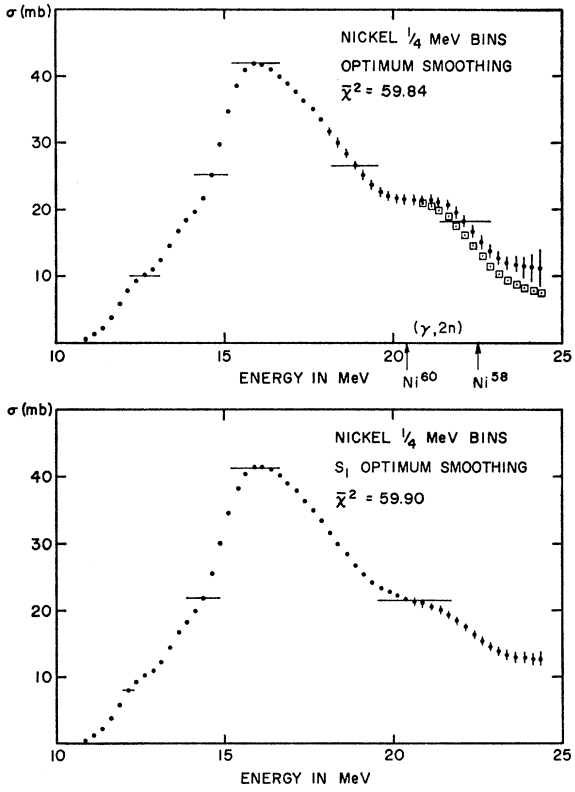

FIG. 1. Least-structure solutions for natural nickel. Upper curve: optimum smoothing using S_2 [Eq. (3b)]; lower curve; optimum smoothing using S_1 [Eq. (3a)].

The data points enclosed by the squares are the cross sections after the corrections were made for the $(\gamma,2n)$ process. This correction was made using the statistical model formula of Blatt and Weisskopf.[11] For both nickel and silver, the fraction of neutrons from direct processes was taken to be 10%.[12,13] The values of the

[11] J. M. Blatt and V. F. Weisskopf, *Theoretical Nuclear Physics* (John Wiley & Sons, Inc., New York, 1952), Chap. 8.

[12] G. S. Mutchler, Ph.D. thesis, Massachusetts Institute of Technology, 1966 (unpublished).

[13] R. G. Baker and K. G. McNeill, Can. J. Phys. 39, 1158 (1961).

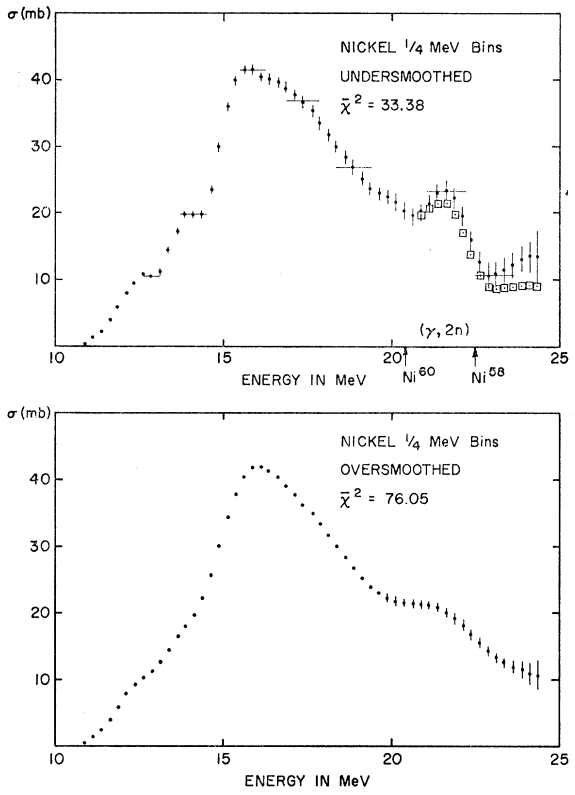

FIG. 2. Least-structure solutions for natural nickel. Upper curve: undersmoothed solution, $x^2=33.38$; lower curve: oversmoothed solution, $x^2=76.05$.

level-density parameter a (Table I) were obtained from the semi-empirical formula $a=A/10.9$ MeV^{-1} (A = mass number) given by Thomson.[14] The cross sections of all the major isotopes were assumed to be equal.

The maximum cross sections σ_m, the energies of the main resonance peaks, E_m, and the integrated cross sections σ_{int} are listed in Table II.

Nickel. In addition to the main giant-resonance peak at 15.9 MeV, the nickel cross section exhibits two smaller peaks at 12.6 and 21.6 MeV. The integrated cross section up to 24 MeV exhausts about 33% of the dipole sum rule, $60(NZ/A)$ MeV mb. The position of the main resonance peak and the integrated cross section agree well with those obtained by Baciu *et al.*[15] In the energy interval covered in this experiment, the neutron-multiplicity correction changes the result very little because of the high $(\gamma,2n)$ thresholds of the nickel isotopes.

TABLE II. Results.

σ_m (mb)	E_m (MeV)	σ_{int} (MeV mb)	Reference
	Nickel [without $(\gamma,2n)$ correction]		
41.9±0.4	15.9	291.1±11(24)[a]	This work
46 ±1	16.5	276 ±25(24)[a]	15
	Silver [with $(\gamma,2n)$ correction]		
181 ±1	16.3	1254(24) [a,b]	This work
240 ±17	16.0	1600(21)[a,b]	16[c]

[a] The numbers in parenthesis are the upper limits of integration for σ_{int}.
[b] Reference 16 gives the cross section of Ag^{107}.
[c] No errors are given with these quantities because of the uncertainty in the neutron multiplicity correction.

Silver. The silver cross section forms a generally smooth curve. The $(\gamma,2n)$ thresholds for the silver isotopes fall very close to the giant resonance peak so the correction for the $(\gamma,2n)$ process narrows the resonance significantly, as shown in Fig. 3. The integrated cross section up to 24 MeV exhausts about 79% of the dipole sum rule.

The values of the peak cross section and the integrated cross section obtained in this experiment for natural silver is about 25% lower than the values obtained by Bogdankevich[16] for the photoneutron cross section of Ag^{107}. Unless there is a systematic error in either measurement, this discrepancy would imply a lower integrated photoneutron cross section and an enhanced proton emission in Ag^{109} than in Ag^{107}.

IV. DISCUSSION

Silver. The predictions of the dynamic collective theory are compared with the experiment in Fig. 3. The theoretical dipole strengths represented by the vertical bars were obtained from Ref. 5, using the average parameters from the low-energy vibrational data[17] of the two neighboring even-even nuclei, Pd^{106} and Cd^{108}. Thus the quadrupole-phonon energy, $E_2=0.57$ MeV, and the mean vibrational amplitude, $\beta_0=0.22$, were used. The positions of the four main dipole levels are all concentrated about the giant-resonance peak and the dipole strength predicted at 19 MeV may correspond to the change of slope observed in the experimental cross section at the same energy. Since the shape of giant resonance in silver is significantly altered by the $(\gamma,2n)$ process, a direct measurement of (γ,n) cross section is desirable for a detailed comparison with any theoretical predictions.

Nickel. The photoneutron cross section of natural nickel shown in Fig. 1 has its main peak at 16 MeV. However, the total photon-absorption cross section for natural nickel, obtained by Wyckoff *et al.*,[18] shows the giant-resonance peak at 19 MeV. This is shown in Fig. 4, where curve A is the total absorption cross section of Ref. 18, and curve C is our experimental photoneutron cross section. Curve B is the difference (A−C), and represents the photoproton cross section in natural nickel. The observed energy separation between the neutron and the proton cross-section peaks in *natural*

[14] D. B. Thomson, Phys. Rev. **129**, 1649 (1963).

[15] G. Baciu, G. C. Bonazzola, B. Minetti, C. Molino, L. Pasqualini, and G. Piraginio, Nucl. Phys. **67**, 178 (1965).

[16] O. V. Bogdankevich, B. I. Goryachev, and V. A. Zapevalov, Zh. Eksperim. i Teor. Fiz. **42**, 1502 (1962) [English transl.: Soviet Phys.—JETP **15**, 1044 (1962)].

[17] M. G. Huber, H. J. Weber, and W. Greiner, Z. Physik **192**, 16 (1966).

[18] J. M. Wyckoff, B. Ziegler, H. W. Koch, and R. Uhlig, Phys. Rev. **137**, B576 (1965).

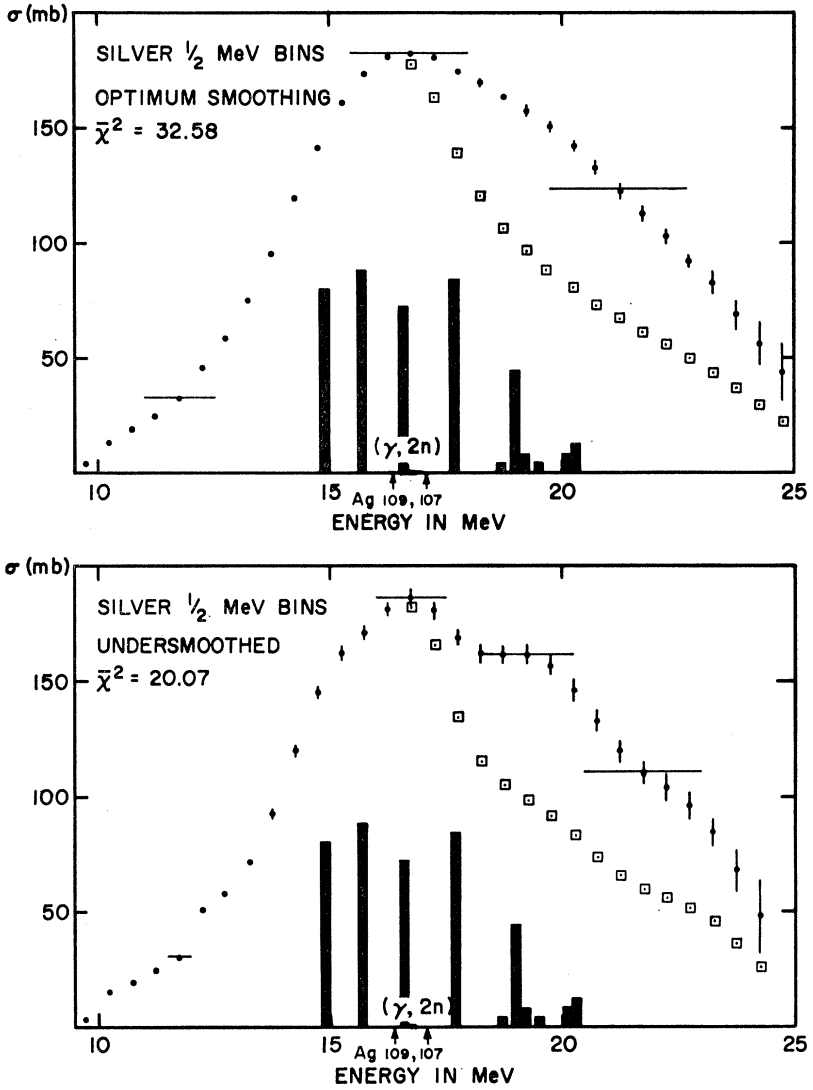

FIG. 3. Least-structure solutions for natural silver. Upper curve: optimum smoothed solution; lower curve: undersmoothed solution, $x^2=20.07$. The vertical bars are the dipole strengths given by the dynamic collective theory (Ref. 5).

nickel implies one of the following possibilities: (1) There is no energy shift between the absorption cross sections of the two major contributing isotopes, Ni^{58} and Ni^{60}. However, the absorption cross section of both isotopes have two peaks at 16 and 19 MeV. In both isotopes, the 16-MeV level decays primarily by neutron emission, while the 19-MeV level decays mainly by proton emission. This is analogous to the observed energy shift in the (γ,n) and (γ,p) cross sections in Zr^{90}, which has been explained by the isobaric splitting between the $\Delta T=0$ and 1 dipole states.[19,20] (2) There is energy shift between the absorption cross sections of Ni^{58} and Ni^{60}. One is peaked at 16 MeV, which decays primarily by neutron emission. The other isotope has its absorption peak at 19 MeV, with suppressed neutron emission.

The available data on the (γ,n) and (γ,p) cross sections of Ni^{58}, measured by Carver and Turchinetz,[21] are consistent with the second of the two assumptions mentioned above. In Fig. 5, curve A is the (γ,n) cross section for natural nickel obtained in this experiment and curve C is the (γ,n) cross section of Ni^{58} of Ref. 19 corrected for its abundance ratio. Curve B is the dif-

TABLE III. Integrated partial cross sections up to 24 MeV for the natural nickel, Ni^{58} and Ni^{60}.

	$\int\sigma_{abs}dE$ (MeV mb)	$\int\sigma(\gamma,n)dE$ (MeV mb)	$\int\sigma(\gamma,p)dE$ (MeV mb)	$\int\sigma(\gamma,p)dE/\int\sigma(\gamma,n)dE$
Natural	650[a]	290	360	1.2
Ni^{58}		180[b]	440[b]	2.4
Ni^{60}		570	160	0.28

[a] Taken from Ref. 18. [b] Taken from Ref. 21.

[19] S. Fallieros, B. Goulard, and R. H. Venter, Phys. Letters **19**, 398 (1965).

[20] V. V. Balashov and E. L. Yadrovsky, Phys. Letters **22**, 509 (1966).

[21] J. H. Carver and W. Turchinetz, Proc. Phys. Soc. (London) **73**, 585 (1959).

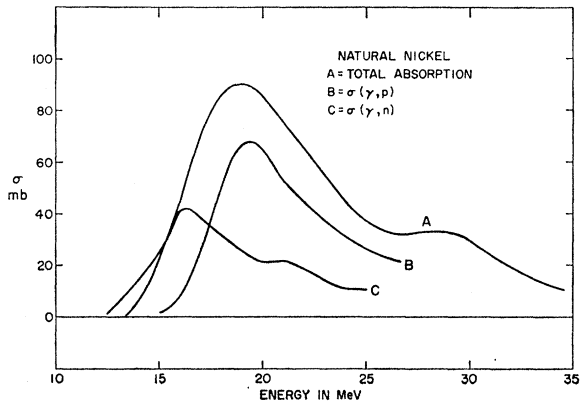

FIG. 4. The total-absorption cross section (Ref. 18) (curve A), the photoneutron cross section (curve C) and the photoproton cross section (curve B = A − C) of natural nickel.

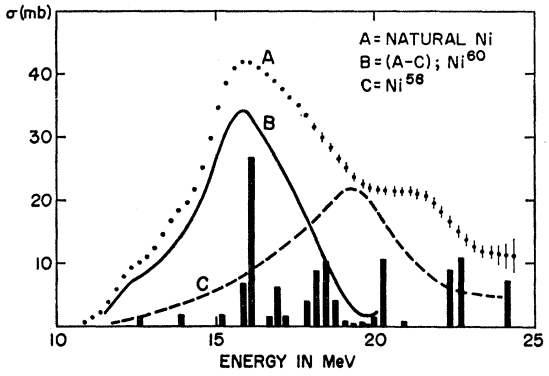

FIG. 5. The photoneutron cross sections for natural nickel (A), Ni^{58} (C, Ref. 21) and Ni^{60} (B = A − C). The vertical bars are the dipole strengths for Ni^{60} given by the collective correlations theory (Ref. 6).

ference (A − C), which represents the Ni^{60} contribution to the (γ,n) cross section. It is seen from Fig. 5 that the main resonance energy for Ni^{60} is 16 MeV compared with the 19-MeV peak of Ni^{58}. According to Ref. 21, Ni^{58} (γ,p) cross section is also peaked at 19 MeV. From Figs. 4 and 5 and the known abundance ratios of Ni^{58} and Ni^{60}, the integrated partial cross sections up to 24 MeV for each isotope were obtained (Table III). The main features of photon absorption in Ni^{58} and Ni^{60} can be summarized as follows: (a) In Ni^{58}, the main absorption is via a level at 19 MeV. Over the whole giant resonance, the ratio $\int\sigma(\gamma,p)dE/\int\sigma(\gamma,n)dE$ is about 2.4. (b) In Ni^{60}, the photon absorption proceeds through a level at 16 MeV. The proton yield is about 30% of the neutron yield.

The anomalously large proton emission rate in Ni^{58} was recently explained by Garfagnini *et al.*[22] to be due to the strong shell effect on the nuclear level density near $N=Z=28$ shells. Using Rosenzwerg's level-density formula,[23] they obtained for Ni^{58} a value of 0.25 for the average ratio of the photoneutron cross section to the total photon-absorption cross section in the energy interval $15<E_\gamma<30$ MeV. Since σ absorption $\cong\sigma(\gamma,n)+\sigma(\gamma,p)$, the calculated ratio $\sigma(\gamma,n)/\sigma_{\text{abs.}}=0.25$ gives the ratio $\sigma(\gamma,p)/\sigma(\gamma,n)=3$. This is in fair agreement with the observed ratio 2.4.

The drastic change in the resonance energies in Ni^{58} and Ni^{60} also suggests a strong shell effect due to the two extra neutrons in Ni^{60}. In Fig. 5, the predicted dipole strengths for Ni^{60} given by the collective correlations theory[6] are shown by the vertical bars. This should be compared with the (γ,n) cross section for Ni^{60}, given by curve B. In the theory of collective correlations, the dipole states are treated in the particle-hole framework while the surface-vibration phonons are treated within the collective model. The agreement with curve B is fairly good. A further test of this theory will be provided by detailed calculations for Ni^{58}, which are not available at present. On the other hand, the difference in the resonance energy between Ni^{58} and Ni^{60}, such as observed in this work, would be difficult to explain in the framework of the dynamic collective theory[5] in which the dipole absorption is treated within the hydrodynamic model, unless vastly different sets of collective parameters are chosen for the two nuclei.

[22] P. Garfagnini, L. Pasqualini, and G. Piragino, Nuovo Cimento **42B**, 290 (1966).
[23] N. Rosenzweig, Phys. Rev. **108**, 817 (1957).